

Peer Reviewed Paper **openaccess**

Application of hyperspectral imaging and chemometrics for classifying plastics with brominated flame retardants

Daniel Caballero,^a Marta Bevilacqua^b and José Manuel Amigo^{c*}

^aChemometrics and Analytical Technology, Department of Food Science, Faculty of Science, Rolighedsvej 26, DK-1958, Frederiksberg C, Denmark and Computer Science Department, Research Institute of Meat and Meat Product (IproCar), University of Extremadura, Av/ Ciencias S/N, ES-10003, Cáceres, Spain. <https://orcid.org/0000-0003-2822-0323>

^bChemometrics and Analytical Technology, Department of Food Science, Faculty of Science, Rolighedsvej 26, DK-1958, Frederiksberg C, Denmark. <https://orcid.org/0000-0002-3361-9219>

^cChemometrics and Analytical Technology, Department of Food Science, Faculty of Science, Rolighedsvej 26, DK-1958, Frederiksberg C, Denmark. E-mail: jmar@food.ku.dk, <https://orcid.org/0000-0003-1319-1312>

Most plastics need to incorporate flame retardants to meet fire safety standards requirements. The amount and the type of flame retardants can differ, so that in waste plastics a large variety of polymers and flame retardants can be found. The recycling of plastics containing flame retardants is increasing. However, only plastics of the same polymer type and the same additive content can be recycled together. Three models based on different chemometrics techniques applied to hyperspectral imaging in the near infrared range were developed [partial least square-discriminant analysis, decision tree (DT) and hierarchical model (HM)]. Optimal results were obtained for all classification techniques. HM shows the highest error at all levels due to the noisy spectra of the black plastics. However, DT classification gave outstanding results, considering that the sensitivity was higher than 0.9 in all cases. Thus, the application of DT with hyperspectral imaging could be used to sort plastic samples with respect to the type of polymer and the flame retardant used with a high degree of accuracy in an automated way. These findings are highly valuable for the plastic and waste management industries.

Keywords: waste recycling, plastics recycling, NIR hyperspectral imaging, polymer, flame retardants, decision tree, hierarchical classification, partial least square-discrimination analysis

Introduction

Most plastics need to incorporate flame retardants (FR) to meet fire safety standard requirements. FRs are organic compounds used to increase the resistance to ignition, reduce flame spreading, suppress smoke formation and prevent a polymer from dripping.¹ The amount and the type of FRs can differ, so that in waste plastics a large variety of polymers and FRs can be found.

Among all, Brominated FRs (BFR) are cost-effective and offer a high degree of processability, making them the most commonly used FRs in plastics. In Europe, the recycling of polymers from all categories is increasing, which includes plastics containing FRs. However, only plastics of the same polymer type and with a close match in additive content can be recycled together.

Correspondence

José Manuel Amigo (jmar@food.ku.dk)

Received: 14 November 2018

Revised: 17 December 2018

Accepted: 4 January 2019

Publication: 22 January 2019

doi: 10.1255/jsi.2019.a1

ISSN: 2040-4565

Citation

D. Caballero, M. Bevilacqua and J.M. Amigo, "Application of hyperspectral imaging and chemometrics for classifying plastics with brominated flame retardants", *J. Spectral Imaging* **8**, a1 (2019). <https://doi.org/10.1255/jsi.2019.a1>

© 2019 The Authors

This licence permits you to use, share, copy and redistribute the paper in any medium or any format provided that a full citation to the original paper in this journal is given, the use is not for commercial purposes and the paper is not changed in any way.



The identification of BFRs in plastics has been successfully accomplished using many methods, such as Raman spectroscopy,² laser-induced breakdown spectrometry (LIBS),³ X-ray fluorescence (XRF)⁴ and chromatography.⁵ However, many of these methods are slow, expensive and difficult to implement in a real-time framework, which make them unsuitable for automated sorting. On the other hand, near infrared (NIR) spectroscopy is extensively used for automated sorting due to its fast scanning abilities and relatively low cost.

Hyperspectral imaging (HSI) is an imaging technique that started in the 1970s with applications mainly in remote sensing.^{6,7} In the last decade, this technique has been applied in many other disciplines.⁸⁻¹⁵ The main feature of this technique is its ability to measure a whole spectrum for every single pixel in which the image (i.e., the sample) is divided.^{16,17} The interest in HSI has recently grown because of the faster, more reliable and robust evolution of the optical devices available and the implementation of powerful, accurate and robust computer vision algorithms for processing those.^{18,19}

HSI is inherently linked to data analysis, especially, to chemometrics techniques. Thus, the success of HSI cannot be understood without referring to the implementation of powerful algorithms to handle all data generated for a single image. Chemometrics is a well-known discipline that allows the extraction of information initially hidden in the data in a multivariate way. Many reviews have been published pointing out the main multivariate or statistical methods that can be applied in HSI for different purposes.²⁰⁻²³ However, sometimes it becomes cumbersome to know exactly which multivariate method is the most appropriate for every single purpose. Among the main chemometrics techniques for classification purposes, partial least square-discriminant analysis (PLS-DA), decision trees (DT) and artificial neural networks (ANN)²⁴⁻²⁷ are very well known.²⁸ Recent studies have shown the good performances in classification of algorithms based on tree structures such as DT or random forest,^{26,29,30} in comparison with classical techniques of classification such as K-NN, rules based systems (RBS), ANN or deep learning methods.

Therefore, a fast and reliable method to identify and distinguish both the polymer and the contained FRs is proposed in this manuscript by using NIR-HSI together with dedicated classification models. This approach can be the perfect methodology for real-time, automated sorting of plastics with critical additives, selecting and

testing the best classification model on real samples of plastics in order to implement an economically reliable recycling process that meets the major requirement of the plastic industry.

Material and methods

Materials

The plastics used in this study were kindly provided by the INNOSORT consortium (<http://innosort.teknologisk.dk/>). Two different kinds of plastics were supplied: *acrylonitrile butadiene styrene* (ABS) and *polystyrene* (PS). For each one, two versions were analysed: *Natural* and *Black* (with the addition of 5% of carbon black). A reference sample for each polymer (without BFRs addition) was analysed and labelled as REF. The remaining samples were doped in the manufacturing process with 10% of different BFRs according to the corresponding legislation. The types of BFR were: *1,2,5,6,9,10-hexabromo-cyclododecane* (labelled as HBCD), *Pentabromophenyl ether* (labelled as deca-BDE) and *3,5-tetrabromobisphenol A* (labelled as TBBPA). These plastics were produced in a disk shape (of around 50mm of diameter and 3mm thickness). For each type of plastic, two replicates were provided, one of them for calibration and the other one for testing (Table 1). Figure 1 shows the false colour image of the samples of plastics (Figure 1A), the use of these images for calibration (black samples) or test (dark grey samples) purposes (Figure 1B) and the identification of each group and subgroup of plastics (Figure 1C). A false colour image is a representation of the hyperspectral image in which the spectra are divided into three intervals. Then, the average value of the spectral signal is calculated for each interval at each pixel. Therefore, a false RGB can be constructed by mimicking each interval as one of the RGB channels. This is a qualitative, but very valuable, way of displaying hyperspectral images. Real samples from commercial sources were used as an external validation set. These were blind random pieces of different types of plastic and from different brands (Figure 2A). The composition of these real plastics are specified in Figure 2B.

Hyperspectral imaging

Images obtained from near infrared reflectance spectroscopy hyperspectral imaging (NIRS-HSI) were collected with the UmBio Inspector hyperspectral camera (UmBio, AB, Umea, Sweden) in the wavelength range

Table 1. Plastic types (ABS, Acrylonitrile Butadiene Styrene and PS, Polystyrene), versions (Natural and Black) and flame retardants (REF, Reference; HBCD, 1,2,5,6,9,10-Hexabromocyclododecane; Deca-BDE, Pentabromophenyl ether; and TBBPA, 3,5-Tetrabromobisphenol A) used in the calibration and test set.

Plastic type	Version	Flame retardants
ABS	Natural	REF
		HBCD
		Deca-BCD
		TBBPA
	Black	REF
		HBCD
		Deca-BCD
		TBBPA
PS	Natural	REF
		HBCD
		Deca-BCD
		TBBPA
	Black	REF
		HBCD
		Deca-BCD
		TBBPA

of 1100–2250 nm with a spectral resolution of 4.85 nm (115 bands). The camera was placed at a right angle with respect to the sample (90°). The samples were illuminated with diffuse white light at an angle of 45° to the sample. The final pixel resolution was 300 μm. This configuration had been evaluated and optimised previously³¹ and the calibration of the camera was performed by subtracting the ratio between the full reflectance of a Spectralon plate and the dark current collected with the objective closed according to the literature.^{32,33}

The hyperspectral image data processing was performed using HYPER-Tools,³⁴ an in-house library working under MATLAB (The Mathworks, Inc., Natick, Massachusetts, USA).

Experimental work-flow

The spectra were pre-processed to remove outliers and noise (first derivative Savitzky–Golay³⁵). The training samples were evaluated and classified by applying three different classification models in a pixel by pixel fashion and analysing sample by sample. Thus, once the best classification model was obtained, this model was evaluated on the NIRS-HSI of the real samples of plastic in

order to evaluate the polymers, the versions and the BFRs doping the plastics of these real samples.

Classification models

Two different datasets were obtained, one for calibration (CAL) and the other for testing the models (TEST). Therefore, to create the calibration model, a matrix \mathbf{X} ($M \times N$) where M is the number of spectra and N is the number of wavelengths, and the corresponding \mathbf{Y} matrix containing the identity belonging to each class,³⁶ are needed.

Partial least square-discriminant analysis

Partial least square (PLS)^{25,37} together with discriminant analysis (PLS-DA) is a supervised discriminant method that predicts whether a sample belongs to a specific class. PLS-DA was performed in the PLS-toolbox (Eigenvector Research Inc., Manson, WA, USA) for MATLAB (The Mathworks Inc., Natick, Massachusetts, USA). This seems a very complicated combination of software. Nevertheless, the two of them (HYPER-Tools and PLS-toolbox) work under the MATLAB environment, and all their utilities can be used in an automated way by means of in-house generated scripts.

Decision trees

DT is a decision modelling tool that graphically displays the classification process of a given input for given output class labels.³⁸ This method is one of the learning algorithms that generate classification models in the form of a tree structure. It is based on the “divide and conquer” strategy.³⁹ Data subsets were created by decomposing the whole dataset into smaller datasets. The final model is a tree structure with decision nodes and leaf nodes.

DT was applied in this study by using the free software Waikato Environment for Knowledge Analysis (WEKA) (<http://www.cs.waikato.ac.nz/ml/weka>; last accessed May 2018).

The J48 decision tree-inducing algorithm is a WEKA implementation of the well-known C4.5 decision tree.⁴⁰ According to Anyanwu and Shiva⁴¹ and Priyam *et al.*,⁴² J48 provides better accuracy and efficiency than other decision tree algorithms. Therefore, J48 was used as the DT in the present study. A confidence factor of 0.5 and minimum bucket size of 30 were applied.^{26,38} The bucket size is the minimum number of samples that can be classified in any leaf of the DT. Usually this value should be one-third of the batch size, which is the number of instances

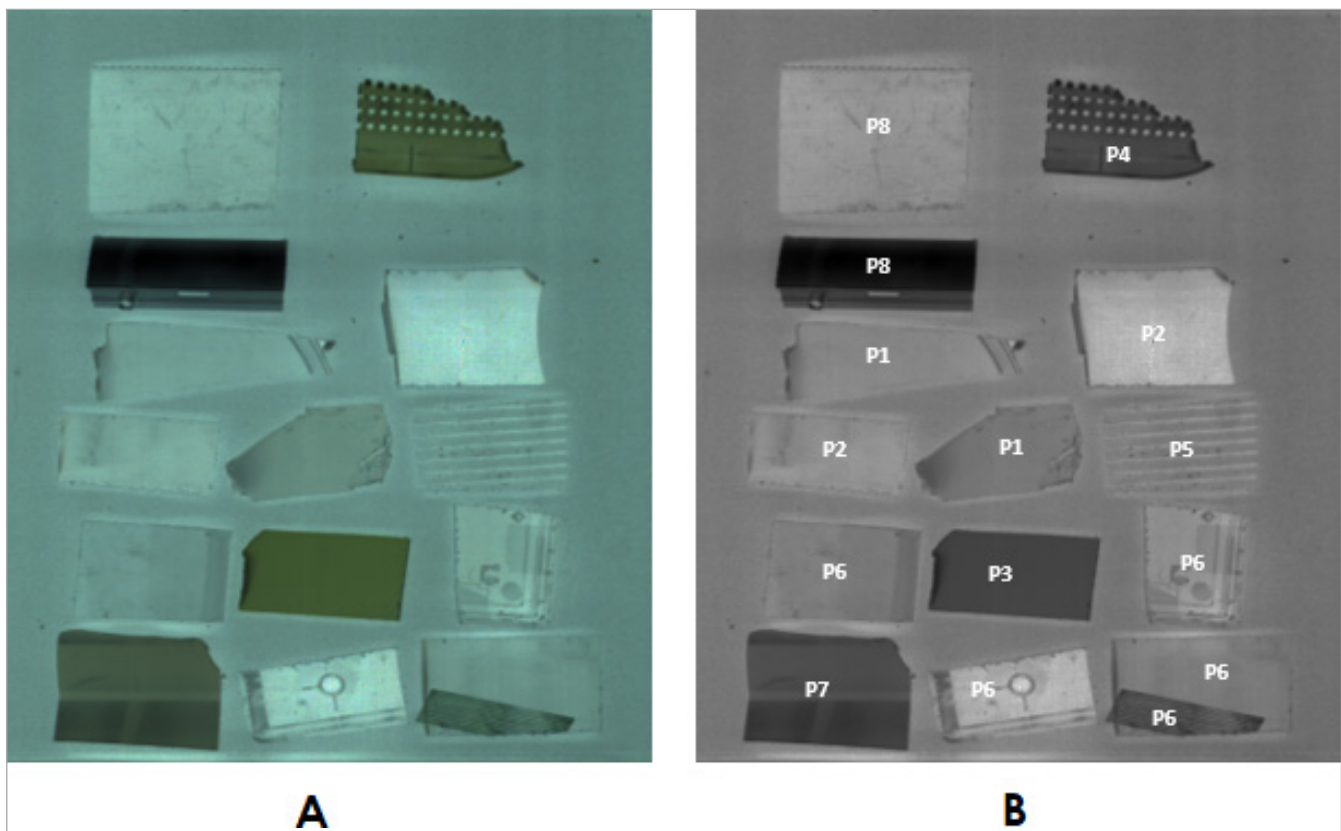
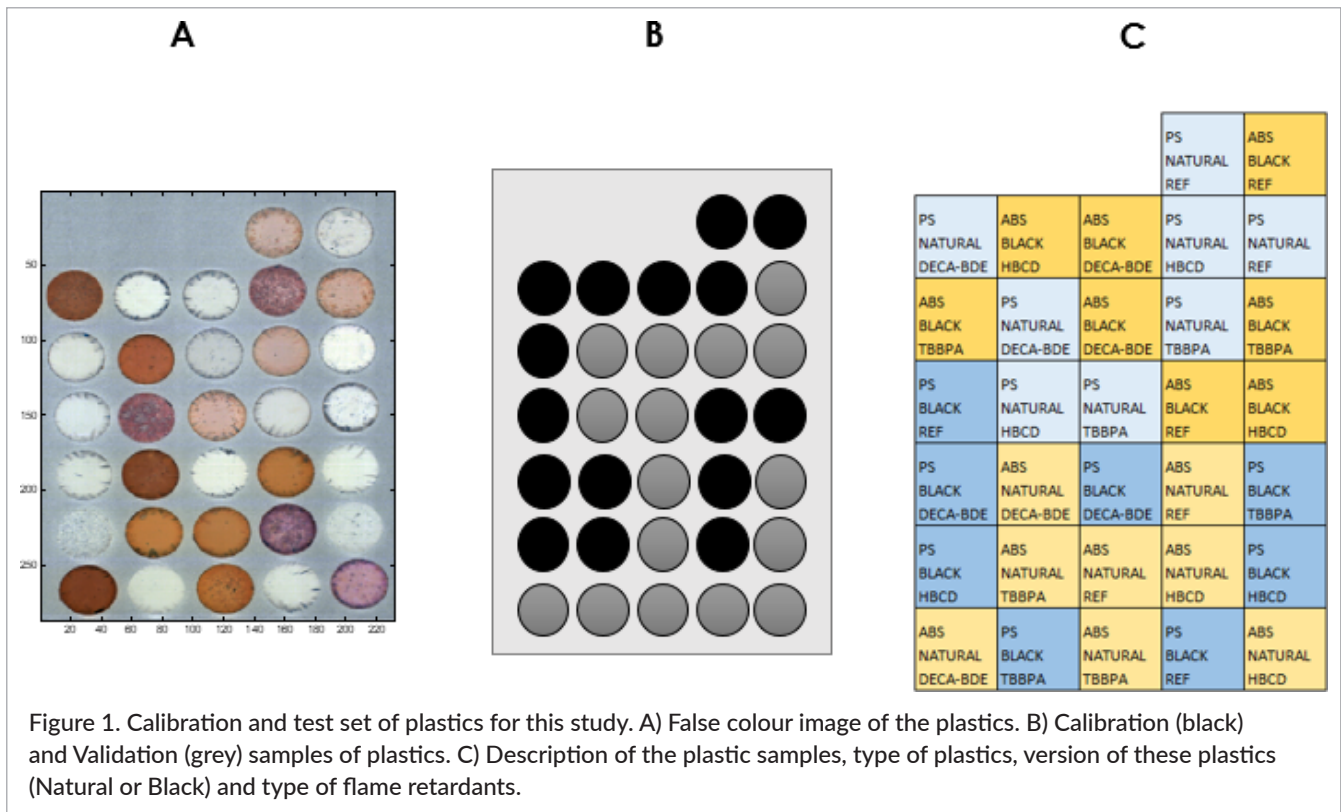


Figure 2. A) False colour image of the real samples of plastics. B) Composition of the real samples of plastics: P1 (ABS-Black-HBCD), P2 (ABS-Black-REF), P3 (ABS-Natural-HBCD), P4 (ABS-Natural-REF), P5 (PS-Black-Deca-BDE), P6 (PS-Black-TBBPA), P7 (PS-Natural-REF) and P8 (PS-Natural-TBBPA).

to process if batch prediction is being performed. Since, the batch size is 100 for the DT, 30 is an appropriate size for the minimum bucket size.

Hierarchical model of classification

A hierarchical model for classifying the plastic samples was developed in the present study. In each level of classification, PLS-DA was applied as the classification technique.³⁷

A hierarchical model of classification is a decision tool that maps the input sample as a function of the output categories. This classification occurs first on a low-level, from highly specific characteristics of the input samples. The classifications of the individual sample are combined systematically, and the sample is classified on a higher level iteratively until one output is produced.^{43,44} This hierarchical model was performed in the PLS-toolbox (Eigenvector Research Inc., Manson, WA, USA) for MATLAB (The Mathworks Inc., Natick, MA, USA).

Statistical assessment of the results

The statistical assessment of the classification performance can also be carried out by using different classifiers.⁴⁵⁻⁴⁷ In our case, the model was statistically evaluated by using the sensitivity (Equation 1), specificity (Equation 2) and class error (Equation 3) for the calibration (CAL) and the test (TEST) sets:

$$\text{Sensitivity} = \frac{TP}{TP + FN} \quad (1)$$

$$\text{Specificity} = \frac{TN}{FP + TN} \quad (2)$$

$$\text{Class error} = 1 - \frac{\text{Sensitivity} + \text{Specificity}}{2} \quad (3)$$

In the equations, TP and TN stand for True Positive and True Negative, respectively, accounting for the pixels that have been correctly assigned as belonging (TP) or not belonging (TN), to a specific class. FP and FN stand for False Positive and False Negative, respectively, accounting for the pixels that have been wrongly assigned as belonging (FP) or not belonging (FN), to a specific class.

Results and discussion

The pre-processed spectra from the different samples are shown in Figure 3. Differences can be seen among

the spectra of different type of polymers, ABS (green spectra) and PS (red spectra). Figure 3B shows differences among the spectra with different versions of plastic, Black (red spectra) and Natural (green spectra). Figure 3C shows differences among the spectra with different FRs used in the plastic, HBCD (green spectra), TBBPA (yellow spectra), Deca-BDE (red spectra) and Reference (blue spectra).

Results from PLS-DA

Table 2 shows the statistical results of the classification models based on PLS-DA built upon the spectral information from each pixel (i.e., classifying pixel by pixel, independently). The best results were obtained for classifying between Natural and Black versions of the plastics, since the classification model obtained a perfect percentage of classification. Good results were obtained for classifying between ABS and PS plastics, since the sensitivity and specificity were higher than 0.75⁴⁸ for the calibration and test sets. For the classification of the FRs used in the plastics, only deca-BDE and TBBPA achieved sensitivity and specificity higher than 0.75⁴⁸ for both calibration and test set. REF and HBCD classes reached sensitivity lower than 0.75 in both sets.⁴⁸ The reason for this performance could be for the high similarity between the spectral features characterising the FRs in the ABS and PS plastics.⁴⁹

The previous results obtained pixel by pixel can then be summarised to classify per sample (i.e., per disk of plastic). In this case, the classification of each sample will be based on the most representative type of plastic, version of plastic and FRs present among the pixels of each specific sample. Table 3 shows these results. The results showed a similar performance of this approach with respect to the one classifying pixel by pixel. The best results were reached for classifying between Black and Natural plastic versions, with all samples classified correctly. For the type of plastic, good results were achieved, except for one PS sample that was wrongly classified as ABS. For the classification among FRs, five samples out of sixteen were wrongly classified.

These results show the ability of linear classification to discriminate between types of plastic and versions of plastic with HSI. Nevertheless, this technique presents problems for discriminating among the FRs added to the plastic, mainly due to the similarity among the spectra of the different FRs.⁴⁹

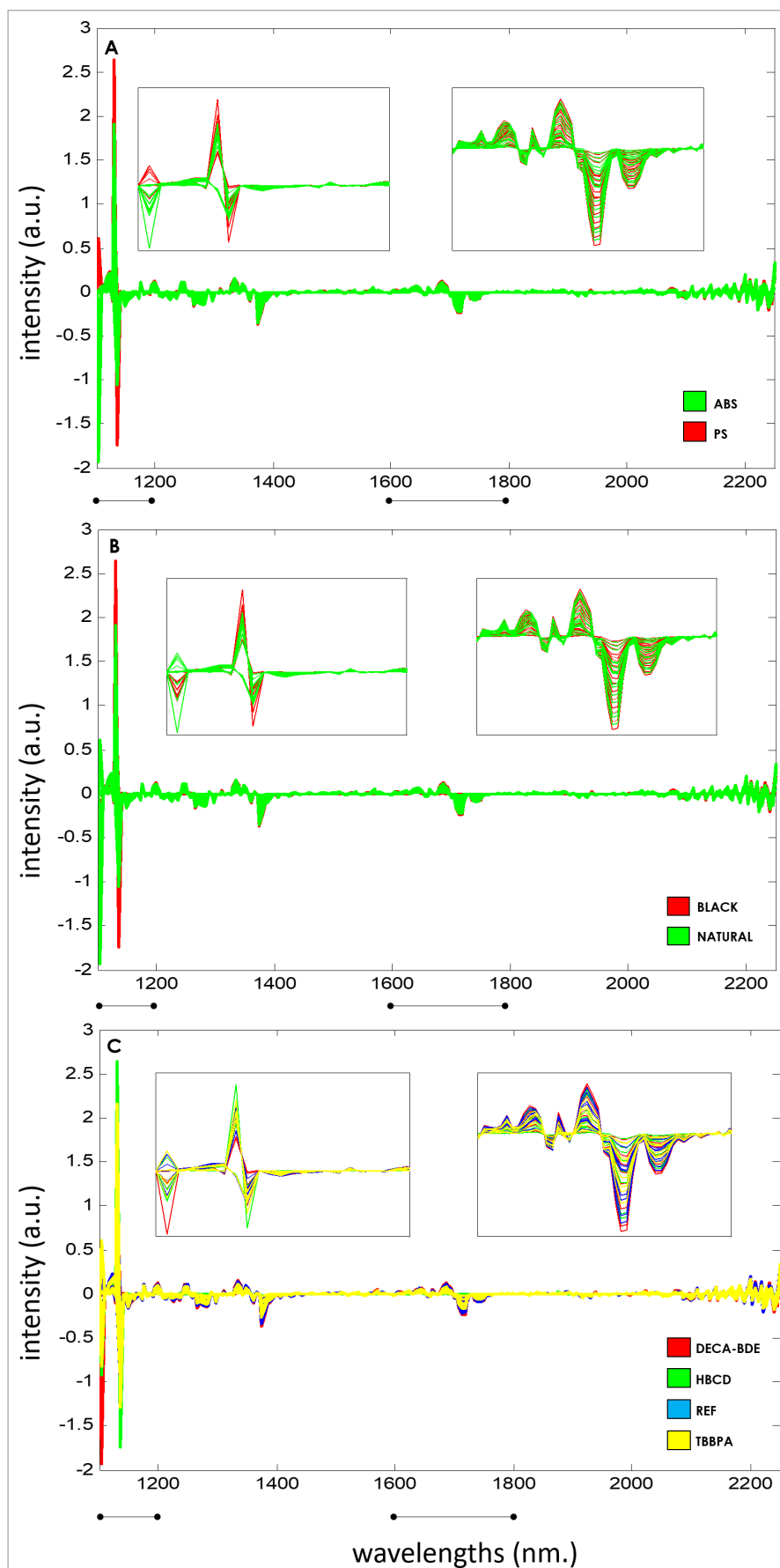


Figure 3. NIRS-HSI for classification of A) type of polymer, PS (red samples) and ABS (blue samples), B) version of plastic, Black (red samples) and Natural (blue samples) and C) type of flame retardant, HBCD (red samples), TBBPA (yellow samples), Deca-BDE (green samples) and REF (blue samples).

Table 2. Results per pixels for the calibration (CAL) and test (TEST) set of plastics using PLS-DA as the chemometrics technique for classifying the type of plastic (ABS, Acrylonitrile Butadiene Styrene and PS, Polystyrene), version (Natural and Black) and flame retardants (REF, Reference; HBCD, 1,2,5,6,9,10-Hexabromo cyclododecane; Deca-BD, Pentabromophenyl ether; and TBBPA, 3,5-Tetrabromobisphenol A).

	Type of plastic		Version		Flame retardants			
	ABS	PS	NATURAL	BLACK	REF	HBCD	Deca-BDE	TBBPA
Sensitivity (CAL)	0.943	0.878	1.000	1.000	0.539	0.709	0.822	0.833
Sensitivity (TEST)	0.941	0.876	1.000	1.000	0.527	0.660	0.760	0.801
Specificity (CAL)	0.878	0.943	1.000	1.000	0.874	0.994	0.869	0.897
Specificity (TEST)	0.876	0.941	1.000	1.000	0.851	0.987	0.860	0.884
Class error (CAL)	0.089	0.089	0.000	0.000	0.294	0.148	0.154	0.134
Class error (TEST)	0.091	0.091	0.000	0.000	0.311	0.176	0.189	0.157

Table 3. Results per sample for the calibration (CAL) and test (TEST) set of plastics using PLS-DA as the chemometrics technique for classifying for the type of plastic (ABS, Acrylonitrile Butadiene Styrene and PS, Polystyrene), version (Natural and Black) and flame retardants (REF, Reference; HBCD, 1,2,5,6,9,10-Hexabromo cyclododecane; Deca-BDE, Pentabromophenyl ether; and TBBPA, 3,5-Tetrabromobisphenol A).

	Type of plastic		Version		Flame retardants			
	ABS	PS	NATURAL	BLACK	REF	HBCD	Deca-BDE	TBBPA
Sensitivity (CAL)	1.000	0.875	1.000	1.000	0.500	0.750	0.750	0.750
Sensitivity (TEST)	1.000	0.875	1.000	1.000	0.500	0.750	0.750	0.750
Specificity (CAL)	0.875	1.000	1.000	1.000	1.000	0.833	0.917	0.833
Specificity (TEST)	0.875	1.000	1.000	1.000	1.000	0.833	0.917	0.833
Class error (CAL)	0.063	0.063	0.000	0.000	0.250	0.208	0.167	0.208
Class error (TEST)	0.063	0.063	0.000	0.000	0.250	0.208	0.167	0.208

Results on decision trees

From all the classification techniques based on tree structures, DT was selected in this work as the classification technique, since DT is one of the simplest tree structures and J48 DT is one of the most efficient algorithms.^{41,42}

Table 4 shows the statistical results of the classification models based on DT using the pixel information one by one. For classifying the types of plastics, very good results were achieved (sensitivity and specificity higher than 0.97 for the calibration sets and higher than 0.96 for the test set). In general, better results were reached for PS than ABS. For classifying the versions of the plastics, very good results were also obtained (sensitivity and specificity higher 0.99 for calibration and test sets). For the FRs, very good results were reached for the calibration and test sets (specificity higher than 0.96, and sensitivity higher than 0.94 for calibration set and higher than 0.93 for test set). Moreover, very good results for the class error were achieved for all cases (lower than 0.05, for the calibration and test sets).

Table 5 shows the results for the classification of the plastics per samples, i.e. classifying disk by disk, as a function of type of plastic, version of plastic and FRs present in the samples. In this case, this approach presents perfect results for all the classification problems.

Results on hierarchical model

A hierarchical classification model was performed. Figure 4 shows the hierarchical classification model described.

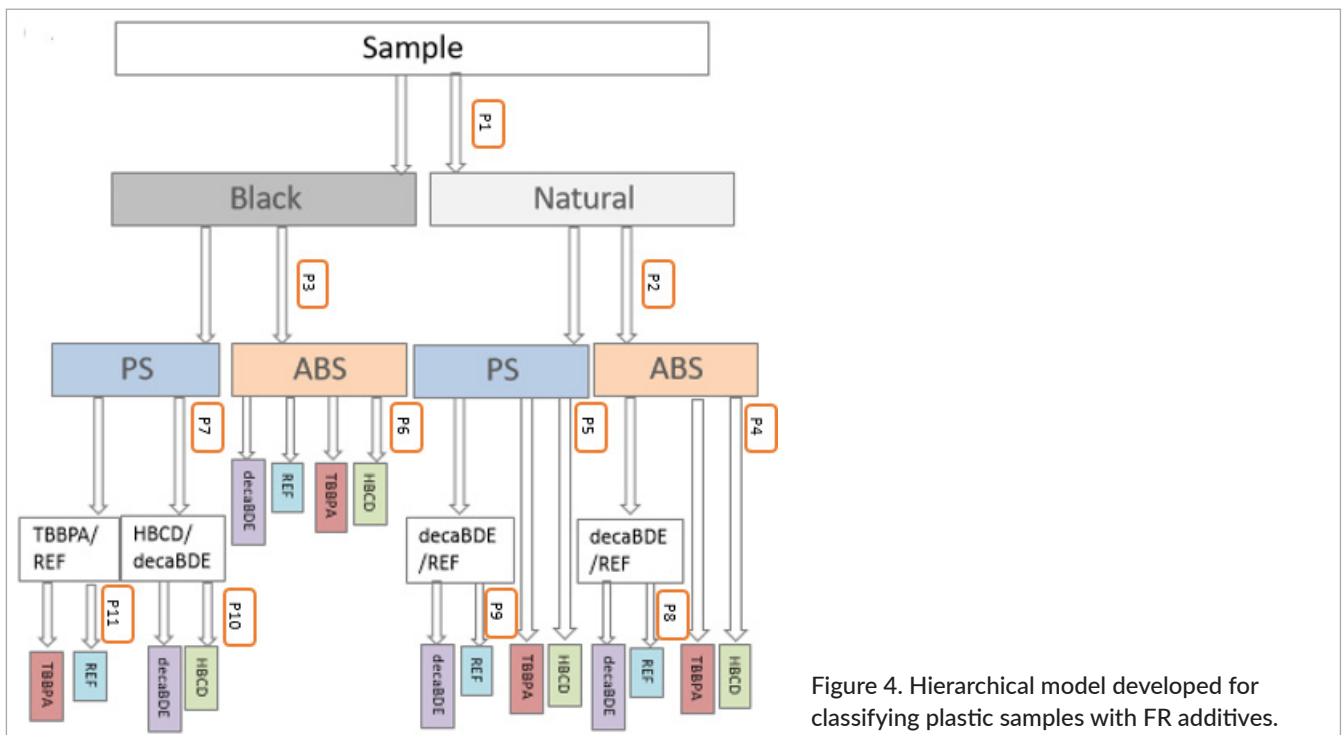
For that, based on the results obtained by the single PLS-DA model (Table 2 and Table 3), the best results were obtained when discriminating between the two versions of the plastics (Natural and Black). For this reason, the classification of the plastics by their versions was chosen as the first PLS-DA model (P1). Once the plastics had been classified as Natural or Black, the next step was to classify them as a function of their polymer (ABS and PS). This step implied two PLS-DA models, one of them for Natural plastics (P2) and the other for Black plastics (P3). At this stage, we had classified four groups

Table 4. Results per pixel for the calibration (CAL) and test (TEST) set of plastics by using DT as the chemometrics technique for classifying the type of plastic (ABS, Acrylonitrile Butadiene Styrene and PS, Polystyrene), version (Natural and Black) and flame retardants (REF, Reference; HBCD, 1,2,5,6,9,10-Hexabromo cyclododecane; Deca-BDE, Pentabromophenyl ether; and TBBPA, 3,5-Tetrabromobisphenol A).

	Type of plastic		Version		Flame retardants			
	ABS	PS	NATURAL	BLACK	REF	HBCD	Deca-BDE	TBBPA
Sensitivity (CAL)	0.976	0.977	0.997	0.998	0.943	0.945	0.965	0.959
Sensitivity (TEST)	0.962	0.964	0.992	0.993	0.937	0.938	0.958	0.951
Specificity (CAL)	0.977	0.976	0.998	0.997	0.973	0.986	0.988	0.991
Specificity (TEST)	0.964	0.962	0.993	0.992	0.968	0.980	0.983	0.985
Class error (CAL)	0.024	0.024	0.003	0.003	0.042	0.035	0.024	0.025

Table 5. Results per sample for the calibration (CAL) and test (TEST) set of plastics by using DT as the chemometrics technique for classifying for type of plastic (ABS, Acrylonitrile Butadiene Styrene and PS, Polystyrene), version (Natural and Black) and flame-retardants (REF, Reference; HBCD, 1,2,5,6,9,10-Hexabromo cyclododecane; Deca-BDE, Pentabromophenyl ether; and TBBPA, 3,5-Tetrabromobisphenol A).

	Type of plastic		Version		Flame retardants			
	ABS	PS	NATURAL	BLACK	REF	HBCD	Deca-BDE	TBBPA
Sensitivity (CAL)	1.000	1.000	1.000	1.000	1.000	1.000	1.000	1.000
Sensitivity (TEST)	1.000	1.000	1.000	1.000	1.000	1.000	1.000	1.000
Specificity (CAL)	1.000	1.000	1.000	1.000	1.000	1.000	1.000	1.000
Specificity (TEST)	1.000	1.000	1.000	1.000	1.000	1.000	1.000	1.000
Class error (CAL)	0.000	0.000	0.000	0.000	0.000	0.000	0.000	0.000



of plastics (NATURAL-ABS, NATURAL-PS, BLACK-ABS and BLACK-PS). Thus, the next step was to classify as a function of the FRs. For the group NATURAL-ABS, we could not build a hierarchical model able to discriminate among all the FRs at once. We had to insert an intermediate step with a model discriminating between HBCD, TBBPA and the remaining FRs (Deca-BDE and REF) (P4). Then, these last samples were classified based on the FRs content, in a following *ad hoc* step (P8). A similar approach was adopted for the group NATURAL-PS where the same problems as in the previous case were encountered. As previously explained, the classification was divided into two subsequent steps, the first one discriminating among HBCD, TBBPA and the remaining FRs (Deca-BDE and REF) (P5), and the second dividing these remaining samples among Deca-BDE and REF (P9). In the case of BLACK-ABS samples, the proposed model discriminated all samples as a function of the FRs at once (P6). Finally, for the BLACK-PS samples, our PLS-DA model discriminated the plastics at first in two sub-groups as a function of FRs contained (P7): one of them with the samples containing HBCD and Deca-BDE as FR, and the other one with the samples containing TBBPA and REF. In both cases, a subsequent PLS-DA model was carried out, to discriminate between HBCD and Deca-BDE (P10) and between TBBPA and REF (P11).

Table 6 shows the statistical results of our hierarchical classification model applied to the data pixel by pixel, and Table 7 shows the same approach applied per sample, i.e. classifying disk by disk.

Very good results (Sensitivity > 0.750)⁴⁸ was obtained for the classification of the plastics according to their version (BLACK and NATURAL) (P1) in both cases (Table 6 and Table 7). The classification as a function of the polymer (ABS and PS) (P2 and P3) led to good classification results with Sensitivity higher than 0.750,⁴⁸ both for the classification by pixel (Table 6) and by sample (Table 7).

For classifying the four classes (BLACK-ABS, BLACK-PS, NATURAL-ABS and NATURAL-PS) according to the specific FRs (P4, P5, P6, P7, P8, P9, P10 and P11), better results were achieved for the Natural plastics than for the Black plastics. For the Natural versions of the plastics (P4, P5, P8 and P9), good results of classification were achieved (Sensitivity > 0.900). However, for the Black versions of the plastics (P6, P7, P10 and P11), the results were not very satisfactory (Sensitivity > 0.500).

This fact could be due to the high noise present in the spectra of the Black plastics where light scattering phenomena occur. This is also true for some of the Natural plastics that appear black due to particular kind of FR used, even if no carbon black was used for their preparation.^{50,51}

Comparing the different models developed in this study, the best results were obtained for the model based on DT (Table 4 and Table 5) following by the results of the hierarchical classification model (Table 6 and Table 7) and the worst results were obtained for PLS (Table 2 and Table 3). These results are in reasonable agreement with previous studies^{26,29,30} that showed the best classification results for tree-structure-based models and the accuracy of classification techniques based on tree structures.

Other studies aimed at classifying plastics⁵²⁻⁵⁴ showed similar performances to the PLS-DA and hierarchical classification model results, therefore inferior to the ones obtained here with the DT approach.

Application on real samples

Once the best classification model was determined, this was applied to the real samples, namely, the different waste plastics of different common brands (Figure 2A), in order to evaluate the polymer used for these plastics, and whether they contained carbon black and FRs (Figure 2B). This is an important step, since this model would be used in recycling processes for the waste recycling and plastic industries that will rely on its accuracy for economic benefits.

At first, the classification model developed in this study was applied on the real samples in order to discriminate between the polymers of the plastics (ABS and PS). Figure 5A illustrates this classification.

The DT model classified the real samples of plastics into ABS samples (blue samples) and PS samples (red samples) correctly. The DT model, classified the different samples and applied the classification model per whole sample.

After that, the DT classification model was applied on the real samples to discriminate between the version of the plastics (BLACK and NATURAL), i.e. for classifying the plastics as a function of whether the plastics contain carbon black. Figure 5B shows this classification.

In Figure 5B, we can see how the DT model classified the real samples of plastics among Black samples (red) and Natural samples (blue). In addition, in this case, the DT model classified the different samples as a whole, and not pixel by pixel, and the results were 100% correct.

Table 6. Results per pixel for the calibration (CAL) and test (TEST) sets of plastics using hierarchical classification model as the chemometrics technique for classifying for the type of plastic (ABS, Acrylonitrile Butadiene Styrene and PS, Polystyrene), version (Natural and Black) and flame retardants (REF, Reference; HBCD, 1,2,5,6,9,10-Hexabromo cyclododecane; Deca-BDE, Pentabromophenyl ether; and TBBPA, 3,5-Tetrabromobisphenol A).

	Classes	Sensitivity (CAL)	Sensitivity (TEST)	Specificity (CAL)	Specificity (TEST)	Class error (CAL)	Class error (TEST)
P1	Natural and Black	1.000	1.000	1.000	1.000	0.000	0.000
P2	Natural → ABS and PS	1.000	1.000	1.000	1.000	0.000	0.000
P3	Black → ABS and PS	0.923	0.903	0.923	0.903	0.077	0.097
P4	Natural → ABS → HBCD, TBBPA and DecaBDE+REF	0.951	0.946	0.973	0.972	0.038	0.041
P5	Natural → PS → HBCD, TBBPA and DecaBDE+REF	0.929	0.916	0.953	0.948	0.059	0.068
P6	Black → ABS → HBCD, TBBPA, DecaBDE and REF	0.837	0.789	0.895	0.833	0.134	0.189
P7	Black → PS → HBCD + DecaBDE and TBBPA + REF	0.924	0.916	0.924	0.916	0.076	0.084
P8	Natural → ABS → DecaBDE and REF	1.000	0.994	1.000	0.994	0.000	0.006
P9	Natural → PS → DecaBDE and REF	0.979	0.972	0.979	0.972	0.021	0.028
P10	Black → PS → HBCD and DecaBDE	0.892	0.882	0.892	0.882	0.108	0.118
P11	Black → PS → TBBPA and REF	0.976	0.976	0.976	0.976	0.024	0.024

Finally, Figure 5C illustrates the DT classification model applied to the real samples to discriminate between the specific FRs used for doping the plastic (HBCD, TBBPA, Deca-BDE and REF).

For this task, again, the DT model analysed the real samples of plastics as whole, not pixel by pixel, and it classified them among REF samples (blue samples), TBBPA

samples (yellow samples), Deca-BDE (green samples) and HBCD samples (red samples). In both cases, we can observe that the FRs used by the plastic industries are in accord with the fire safety standard required. Once again, the DT model classified the different samples 100% correctly as a function of the FRs for doping the plastics.

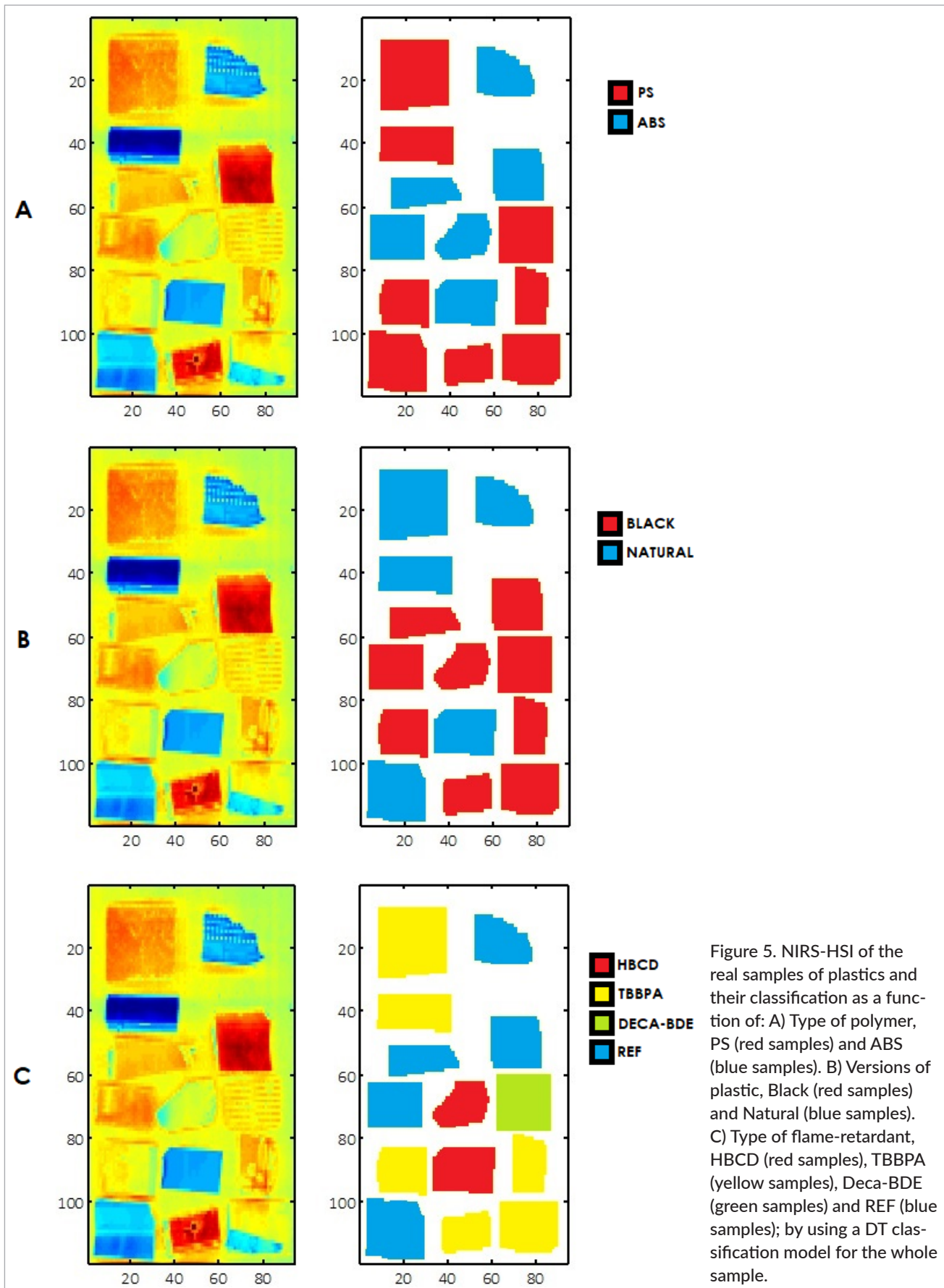
Table 7. Results per sample for the calibration (CAL) and test (TEST) set of plastics using hierarchical classification model as the chemometrics technique for classifying the type of plastic (ABS, Acrylonitrile Butadiene Styrene and PS, Polystyrene), version (Natural and Black) and flame retardants (REF, Reference; HBCD, 1,2,5,6,9,10-Hexabromo cyclododecane; Deca-BDE, Pentabromophenyl ether; and TBBPA, 3,5-Tetrabromobisphenol A).

	Classes	Sensitivity (CAL)	Sensitivity (TEST)	Specificity (CAL)	Specificity (TEST)	Class error (CAL)	Class error (TEST)
P1	Natural and Black	1.000	1.000	1.000	1.000	0.000	0.000
P2	Natural → ABS and PS	1.000	1.000	1.000	1.000	0.000	0.000
P3	Black → ABS and PS	0.875	0.750	0.875	0.750	0.125	0.250
P4	Natural → ABS → HBCD, TBBPA and DecaBDE+REF	1.000	0.750	1.000	0.750	0.000	0.250
P5	Natural → PS → HBCD, TBBPA and DecaBDE+REF	1.000	0.750	1.000	0.750	0.000	0.250
P6	Black → ABS → HBCD, TBBPA, DecaBDE and REF	0.750	0.500	0.750	0.500	0.250	0.500
P7	Black → PS → HBCD + DecaBDE and TBBPA + REF	0.500	0.250	0.500	0.250	0.500	0.750
P8	Natural → ABS → DecaBDE and REF	1.000	0.500	1.000	1.000	0.000	0.000
P9	Natural → PS → DecaBDE and REF	1.000	1.000	1.000	1.000	0.000	0.000
P10	Black → PS → HBCD and DecaBDE	0.500	0.500	0.500	0.500	0.500	0.500
P11	Black → PS → TBBPA and REF	0.500	0.500	0.500	0.500	0.500	0.500

Conclusions

Three classification models were developed in this study based on the combination of chemometrics techniques and HSI. All, these methods were suitable for classifying the plastic samples, but the best results were achieved with DT as the classification technique.

The results indicate that the application of DT with HSI could be used for sorting plastic samples with respect to their type of plastic (polymer), version of plastics (colour) and the FRs used for doping the plastic, with a high degree of accuracy and in an automated way. These findings are highly valuable for the plastic industries and for the waste recycling industries. These results are even



more remarkable, considering that the applications of the models on real samples, led to correct classification of 100%, notwithstanding the differences in texture, shape and orientation of these last samples.

Therefore, a new method, fast, robust and reliable to identify and distinguish the polymers and the contained substances could be of high value to the plastic and waste recycling industries, saving both time and money.

Acknowledgements

Daniel Caballero thanks the “Junta de Extremadura” for a post-doctoral grant (PO17017). This manuscript has been possible thanks to the financial support received from the INNOSORT project. The plastics used in this study were kindly provided by the INNOSORT consortium. INNOSORT is a consortium that brings together technology suppliers, research and knowledge institutions and recipients of waste separation techniques and separated materials. See further information about INNOSORT and partners at <http://innosort.teknologisk.dk/>.

Abbreviations

FR: Flame Retardants. BFR: Brominated Flame Retardants. LIBS: Laser-Induced Breakdown Spectrometry. XRF: X-Ray Fluorescence. NIRS: Near Infrared Reflectance Spectroscopy. HSI: Hyperspectral Imaging. PLS-DA: Partial Least Square-Discriminant Analysis. DT: Decision Trees. ANN: Artificial Neural Networks. RBS: Rules Based Systems. ABS: Acrylonitrile Butadiene Styrene. PS: Polystyrene. REF: Reference. HBCD: 1,2,5,6,9,10-hexabromo-cyclododecane. Deca-BDE: Pentabromophenyl ether. TBBPA: 3,5-tetrabromobisphenol A. NIRS-HSI: Near Infrared Reflectance Spectroscopy Hyperspectral Images. SNV: Standard Normal Variate. CAL: Calibration Set. TEST: Test Set. PLS: Partial Least Square. WEKA: Waikato Environment for Knowledge Analysis. TP: True Positive. TN: True Negative. FP: False Positive. FN: False Negative. K-NN: K-Nearest Neighbours.

References

1. C.A. De Wit, “An overview of brominated flame retardants in the environment”, *Chemosphere* **46**, 583–624 (2002). [https://doi.org/10.1016/S0045-6535\(01\)00225-9](https://doi.org/10.1016/S0045-6535(01)00225-9)
2. S. Kikuchi, K. Kawachi, S. Ooki, M. Kurosawa, H. Honjho and T. Yagishita, “Non-destructive rapid analysis of brominated flame retardants in electrical and electronic equipment using Raman spectroscopy”, *Anal. Sci.* **20**, 1111–1112 (2004). <https://doi.org/10.2116/analsci.20.1111>
3. M. Stepputat and R. Noll, “On-line detection of heavy metals and brominated flame retardants in technical polymers with laser-induced breakdown spectrometry”, *Appl. Optics* **42**, 6210–6220 (2003). <https://doi.org/10.1364/AO.42.006210>
4. C. Gallen, A. Banks, S. Brandsma, C. Baduel, P. Thai, G. Eaglesham, A. Hefferman, P. Leonards, P. Bainton and J.F. Mueller, “Towards development of a rapid and effective non-destructive testing strategy to identify brominated flame retardants in the plastics of consumer products”, *Sci. Total Environ.* **491**, 255–265 (2014). <https://doi.org/10.1016/j.scitotenv.2014.01.074>
5. M. Schlummer, F. Brandl, A. Maurer and R. Van Eldik, “Analysis of flame retardant additives in polymer fractions of waste of electric and electronic equipment (WEEE) by means of HPLC-UV/MS and GPC-HPLC-UV”, *J. Chromatogr. A* **1064**, 39–51 (2005). <https://doi.org/10.1016/j.chroma.2004.12.016>
6. C.A. Lee, S.D. Gasster, A. Plaza, C.I. Chang and B. Huang, “Recent developments in high performance computing for remote sensing: a review”, *IEEE J. Select. Topics Appl. Earth Observ. Remote Sens.* **4**, 508–527 (2011). <https://doi.org/10.1109/JSTARS.2011.2162643>
7. R.A. Schowengerdt, *Remote Sensing*, 3rd Edn. Elsevier, Amsterdam, Netherlands (2006).
8. J.M. Amigo, J. Cruz, M. Bautista, S. Maspocho, J. Coello and M. Blanco, “Study of pharmaceutical samples by NIR chemical-image and multivariate analysis”, *TrAC—Trends Anal. Chem.* **27**, 696–713 (2008). <https://doi.org/10.1016/j.trac.2008.05.010>
9. J.M. Amigo, “Practical issue of hyperspectral imaging analysis of solid dosage forms”, *Anal. Bioanal. Chem.* **398**, 93–109 (2010). <https://doi.org/10.1007/s00216-010-3828-z>
10. J.M. Amigo, I. Marti and A. Gowen, “Hyperspectral imaging and chemometrics, a perfect combination for the analysis of food structure, composition and quality”, *Data Handl. Sci. Technol.* **28**, 343–370

- (2013). <https://doi.org/10.1016/B978-0-444-59528-7.00009-0>
11. M.T.F. De la Ossa, C. García-Ruiz and J.M. Amigo, "Near infrared spectral imaging for the analysis of dynamite residues on human handprints", *Talanta* **130**, 315–321 (2014). <https://doi.org/10.1016/j.talanta.2014.07.026>
 12. T.M. Karlsson, H. Grhan, B. van Bavel and P. Geladi, "Hyperspectral imaging and data analysis for detecting and determining plastic contamination in seawater filtrates", *J. Near Infrared Spectrosc.* **24**, 141–149 (2016). <https://doi.org/10.1255/jnirs.1212>
 13. M.E. Klein, B.J. Aalderink, R. Padoan, G. De Bruin and T.A.G. Steemers, "Quantitative hyperspectral reflectance imaging", *Sensors* **8**, 5576–5618 (2008). <https://doi.org/10.3390/s8095576>
 14. G.L. Lu and B.W. Fei, "Medical hyperspectral imaging: a review", *J. Biomed. Opt.* **19**, 10901 (2014). <https://doi.org/10.1117/1.JBO.19.1.010901>
 15. D.W. Sun, *Hyperspectral Imaging for Food Quality Analysis and Control*. Elsevier, Amsterdam, Netherlands (2010).
 16. C.-M. Wang, S.-C. Yang, P.-C. Chung, C.-I. Chang, C.-S. Lo, C.-C. Chen, C.-W. Yang and C.-H. Wen, "Orthogonal subspace projection-based approaches to classification of MR image sequences", *Comput. Med. Imag. Graph.* **25**, 465–476 (2001). [https://doi.org/10.1016/S0895-6111\(01\)00015-5](https://doi.org/10.1016/S0895-6111(01)00015-5)
 17. Z.M. Xu and E.Y. Lam, "Image reconstruction using spectroscopic and hyperspectral information for compressive terahertz imaging", *J. Opt. Soc. Amer. A* **27**, 1638–1646 (2010). <https://doi.org/10.1364/JOSAA.27.001638>
 18. D. Caballero, A. Caro, A.B. Dahl, B.K. Ersboll, J.M. Amigo, T. Pérez-Palacios and T. Antequera, "Comparison of different image analysis algorithms on MRI to predict physico-chemical and sensory attributes of loin", *Chemometr. Intell. Lab. Syst.* **180**, 54–63 (2018). <https://doi.org/10.1016/j.chemo-lab.2018.04.008>
 19. S. Cubero, N. Aleixos, E. Moltó, J. Gómez-Sanchis and J. Blasco, "Advances in machine vision application for automatic inspection and quality evaluation of fruits and vegetables", *Food Bioproc. Technol.* **4**, 487–504 (2011). <https://doi.org/10.1007/s11947-010-0411-8>
 20. C.I. Chang, X. Jiao, C.C. Wu, Y. Du and M.L. Chang, "A review of unsupervised spectral target analysis for hyperspectral imagery", *Eurasip J. Adv. Signal Proc.* **2010**, 503752 (2010). <https://doi.org/10.1155/2010/503752>
 21. D.M. Haaland, H.D.T. Jones, M.H. Van Benthem, M.B. Sinclair, D.K. Melgaard, C.L. Stork, M.C. Pedroso, P. Liu, A.R. Brasier, N.I. Andrews and D.S. Lidke, "Hyperspectral confocal fluorescence imaging: exploring alternative multivariate curve resolution approaches", *Appl. Spectrosc.* **63**, 271–279 (2009). <https://doi.org/10.1366/000370209787598843>
 22. J.A.F. Pierna, P. Vermeulen, O. Amand, A. Tossens, P. Dardenne and V. Baeten, "NIR hyperspectral imaging spectroscopy and chemometrics for the detection of undesirable substances in food and feed", *Chemometr. Intell. Lab. Syst.* **117**, 233–239 (2012). <https://doi.org/10.1016/j.chemo-lab.2012.02.004>
 23. M. Vidal and J.M. Amigo, "Pre-processing of hyperspectral images. Essential steps before image analysis", *Chemometr. Intell. Lab. Syst.* **117**, 138–148 (2012). <https://doi.org/10.1016/j.chemolab.2012.05.009>
 24. D. Ballabio and M. Vasighi, "A MATLAB toolbox for self organizing maps and supervised neural network learning strategies", *Chemometr. Intell. Lab. Syst.* **118**, 24–32 (2012). <https://doi.org/10.1016/j.chemo-lab.2012.07.005>
 25. R. Bro, "Multiway calibration. Multilinear PLS", *J. Chemometr.* **10**, 47–61 (1996). [https://doi.org/10.1002/\(SICI\)1099-128X\(199601\)10:1<47::AID-CEM400>3.0.CO;2-C](https://doi.org/10.1002/(SICI)1099-128X(199601)10:1<47::AID-CEM400>3.0.CO;2-C)
 26. D. Caballero, A. Caro, P.G. Rodríguez, M.L. Durán, M.M. Ávila, R. Palacios, T. Antequera and T. Pérez-Palacios, "Modeling salt diffusion in Iberian ham by applying MRI and data mining", *J. Food Eng.* **189**, 115–122 (2016). <https://doi.org/10.1016/j.jfood-eng.2016.06.003>
 27. T. Pérez-Palacios, D. Caballero, A. Caro, P.G. Rodríguez and T. Antequera, "Applying data mining and computer vision techniques to MRI to estimate quality traits in Iberian hams", *J. Food Eng.* **131**, 82–88 (2014). <https://doi.org/10.1016/j.jfood-eng.2014.01.015>
 28. T.M. Mitchell, "Machine learning and data mining", *Commun. ACM* **42**, 30–36 (1999). <https://doi.org/10.1145/319382.319388>
 29. E. Cernadas, M. Fernández-Delgado, E. González-Rufino and P. Carrión, "Influence of normalization

- and color space to color texture classification”, *Pattern Recogn.* **61**, 120–138 (2017). <https://doi.org/10.1016/j.patcog.2016.07.002>
30. M. Fernández-Delgado, E. Cernadas, S. Barro and D. Amorim, “Do we need hundreds of classifiers to solve real world classification problems?”, *J. Mach. Learn. Res.* **15**, 3133–3181 (2014).
31. M. Bevilacqua and J.M. Amigo, “Classification of plastics containing brominated flame retardant through hyperspectral imaging and chemometrics”, in *17th International Conference on Near Infrared Spectroscopy*. Foz do Iguassu, Brazil (2015).
32. J. Burger and P. Geladi, “Hyperspectral NIR image regression part I: calibration and correction”, *J. Chemometr.* **19**, 355–363 (2005). <https://doi.org/10.1002/cem.938>
33. J. Burger and P. Geladi, “Hyperspectral NIR image regression part II: dataset preprocessing diagnostics”, *J. Chemometr.* **20**, 106–119 (2006). <https://doi.org/10.1002/cem.986>
34. N. Mobaraki and J.M. Amigo, “HYPER-Tools. A graphical user-friendly interface for hyperspectral image analysis”, *Chemometr. Intell. Lab. Syst.* **172**, 174–187 (2018). <https://doi.org/10.1016/j.chemo-lab.2017.11.003>
35. A. Rinnan, F. Van der Berg and S.B. Engelsen, “Review of most common pre-processing techniques for near-infrared spectra”, *TrAC—Trends Anal. Chem.* **28**, 1201–1222 (2009). <https://doi.org/10.1016/j.trac.2009.07.007>
36. J.M. Amigo and C. Ravn, “Direct quantification and distribution assessment of major and minor components in pharmaceutical tablets by NIR-chemical imaging”, *Eur. J. Pharm. Sci.* **37**, 76–82 (2009). <https://doi.org/10.1016/j.ejps.2009.01.001>
37. M. Barker and W. Rayens, “Partial least squares for discrimination”, *J. Chemometr.* **17**, 166–173 (2003). <https://doi.org/10.1002/cem.785>
38. S. Drazin and M. Montag, *Decision Tree Analysis Using WEKA*. Machine Learning Project II, University of Miami, Miami, Florida, USA (2012).
39. R. Safavian and D. Landgrebe, “A survey of decision tree classifier methodology”, *IEEE Trans. Syst. Man Cybernet.* **21**(3), 660–674 (1991). <https://doi.org/10.1109/21.97458>
40. R. Quinlan, *C4.5: Programs for Machine Learning*. Morgan Kaufmann Publishers, San Mateo, CA, USA (1993).
41. M.N. Anyanwu and S.G. Shiva, “Comparative analysis of serial decision tree classification algorithms”, *Int. J. Comput. Sci. Secur.* **3**, 230–240 (2009).
42. A. Priyam, G.R. Abhijeeta, A. Rathee and S. Srivastava, “Comparative analysis of decision tree classification algorithms”, *Int. J. Curr. Eng. Technol.* **3**(2), 334–337 (2013).
43. A. Demaid, V. Spedding and J. Zucker, “Classification of plastics materials”, *Artif. Intell. Eng.* **10**(1), 9–20 (1996). [https://doi.org/10.1016/0954-1810\(95\)00012-7](https://doi.org/10.1016/0954-1810(95)00012-7)
44. S.S. Tratch and N.S. Zefirov, “A hierarchical classification scheme for chemical reactions”, *J. Chem. Inf. Modell.* **38**(3), 349–366 (1998).
45. J. Demsar, “Statistical comparisons of classifiers over multiple data sets”, *J. Mach. Learn. Res.* **7**, 1–30 (2006).
46. D.J. Hand, “Assessing the performance of classification methods”, *Int. Stat. Rev.* **80**, 400–414 (2012). <https://doi.org/10.1111/j.1751-5823.2012.00183.x>
47. D. Lorente, J. Blasco, A.J. Serrano, E. Soria-Olivas, N. Aleixos and J. Gómez-Sanchis, “Comparison of ROC feature selection method for the detection of decay in citrus fruit using hyperspectral images”, *Food Bioproc. Technol.* **6**, 3613–3619 (2013). <https://doi.org/10.1007/s11947-012-0951-1>
48. A.P. Hearty and M.J. Gibney, “Analysis of meal patterns with use of supervised data mining techniques—artificial neural networks and decision trees”, *Amer. J. Clin. Nutr.* **88**, 1632–1642 (2008). <https://doi.org/10.3945/ajcn.2008.26619>
49. J.M. Amigo, H. Babamoradi and S. Elcoroaristizabal, “Hyperspectral image analysis. A tutorial”, *Anal. Chim. Acta* **896**, 34–51 (2015). <https://doi.org/10.1016/j.aca.2015.09.030>
50. C.F. Bohren and D.R. Huffman, *Absorption and Scattering of Light by Small Particles*. John Wiley & Sons, Weinheim, Germany (1998). <https://doi.org/10.1002/9783527618156>
51. H. Martens, J.P. Nielsen and S.B. Engelsen, “Light scattering and light absorbance separated by extended multiplicative signal correction application to near-infrared transmission analysis of powder mixtures”, *Anal. Chem.* **75**(3), 394–404 (2003). <https://doi.org/10.1021/ac020194w>
52. F. Hollstein, M. Wohllebe, S. Arnaiz and D. Manjon, *Identification of Bio-Plastics by NIR-SWIR-Hyperspectral-Imaging*. International Conference on

Optical Characterization of Materials, Karlsruhe, Germany (2015).

53. H. Kim and S. Kim, *Band Selection for Plastic Classification Using NIR Hyperspectral Image*. International Conference on Control, Automation and Systems, Gyeongju, South Korea (2016). <https://doi.org/10.1109/ICCAS.2016.7832335>
54. M. Vidal, A. Gowen and J.M. Amigo, "NIR hyperspectral imaging for plastics classification", *NIR news* 23(1), 13 (2015). <https://doi.org/10.1255/nirn.1285>